Catalyst Design

DOI: 10.1002/anie.201301864

Noncovalent Interactions in Organocatalysis: Modulating Conformational Diversity and Reactivity in the MacMillan Catalyst**

Mareike C. Holland, Shyeni Paul, W. Bernd Schweizer, Klaus Bergander, Christian Mück-Lichtenfeld, Sami Lakhdar, Herbert Mayr, and Ryan Gilmour**

Dedicated to Professor Dr. Jack D. Dunitz FRS on the occasion of his 90th birthday.

Organocatalysts are inimitable in both their structural mimicry of enzymatic systems and the activation modes by which they operate.[1] Much can be gleaned from studies of more complex, yet related, biomolecules and the noncovalent interactions that modulate their conformational dynamics and function.[2] Accordingly, the burgeoning field of organocatalysis is uniquely placed to benefit from the maturity of supramolecular and bio-organic chemistry,[3] and enantioselective catalysis to provide innovative solutions to long-standing problems in organic synthesis.[4] This juxtaposition facilitates the development of highly selective reactions proceeding via well-defined intermediates by direct application of stabilizing structural features that are well described in proteins; pertinent examples include CH–π and π–π interactions and hydrogen bond networks. Many of these quintessential characteristics are prominent in secondary amine organocatalysts; the phenylalanine-derived MacMillan catalyst (Figure 1) is an excellent example.[5] The iminium ensemble that is generated by the union of this imidazolidinone and an α,β-unsaturated aldehyde exhibits the same CH–π[6] and π–π interactions[7] as those found in proteins. These intramolecular, noncovalent interactions have been detected spectroscopically and/or crystallographically, and validated by computation in a range of MacMillan-type iminium salts.[8,9] Particularly noteworthy is the propensity of

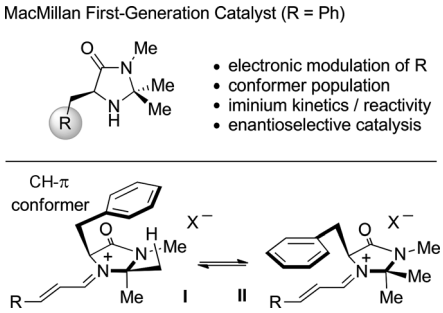

Figure 1. The first-generation imidazolidinone reported by MacMillan and co-workers in 2000.[5]

the phenylalanine side chain to participate in a CH–π interaction with the *syn* methyl group of the catalyst core (**I**; Figure 1): this interaction is found ubiquitously in numerous enzyme structures.[6] Indeed, the system is geometrically predisposed to allow for it, making imidazolidinone-derived iminium salts valuable intermediates for fundamental physical organic studies of this type of interaction.[10] Moreover, there is ample support for a second low-energy conformation where the aryl ring shields the pendant iminium chain (**II**; Figure 1).[11] The role of these interactions in influencing conformation and reactivity in organocatalytic reactions requires clarification. Herein, we report the consequence of electronic modulation of the aromatic group on the conformation and reactivity of α,β-unsaturated MacMillan-type iminium salts. The ground-state conformational studies are complemented by a reactivity and catalysis study, thus illustrating the importance of the aryl group electronics on catalyst performance.

The covalent nature of the organocatalytic intermediates allows for the isolation and characterization of these ensembles as part of the reaction design process. This notion of deconstructing reactions has been successfully applied on several occasions.[12] Initially, the iminium salts (**1**–**6**)·ClO_4^- were prepared to generate a platform from which to begin this investigation, and synthesized from the constituent secondary amines and *trans*-cinnamaldehyde. The electronic nature of the aryl group is reflected by the component of the traceless quadrupole moment tensor orthogonal to the aromatic ring (Q_{ZZ}) calculated for the corresponding toluene derivative ($ArCH_3$) for simplicity (Figure 2; **2**→**6**, Q_{ZZ} 3.01→−5.68). In general, the addition of electron-withdrawing groups renders this number more positive, whilst electron-donating groups have the opposite effect. This can be clearly visualized by an

[*] M. C. Holland, Dr. K. Bergander, Dr. C. Mück-Lichtenfeld, Prof. Dr. R. Gilmour
Organisch Chemisches Institut
Westfälische Wilhelms-Universität Münster
Corrensstrasse 40, 48149 Münster (Germany)
E-mail: ryan.gilmour@uni-muenster.de
Homepage: http://www.uni-muenster.de/Chemie.oc/gilmour/
M. C. Holland, Dr. W. B. Schweizer
Laboratorium für Organische Chemie
ETH Zürich (Switzerland)
S. Paul, Prof. Dr. H. Mayr
Department Chemie
Ludwig-Maximilians-Universität München (Germany)
Dr. S. Lakhdar
Laboratoire de Chimie Moléculaire et Thio-organique, ENSICAEN
6 Boulevard Maréchal Juin, 14050 Caen (France)
E-mail: sami.lakhdar@ensicaen.fr

[**] We acknowledge generous financial support from the WWU Münster, the DFG (SFB 749), and the ETH Zürich (ETH Independent Investigator Research Award to R.G.).

Supporting information for this article is available on the WWW under http://dx.doi.org/10.1002/anie.201301864.

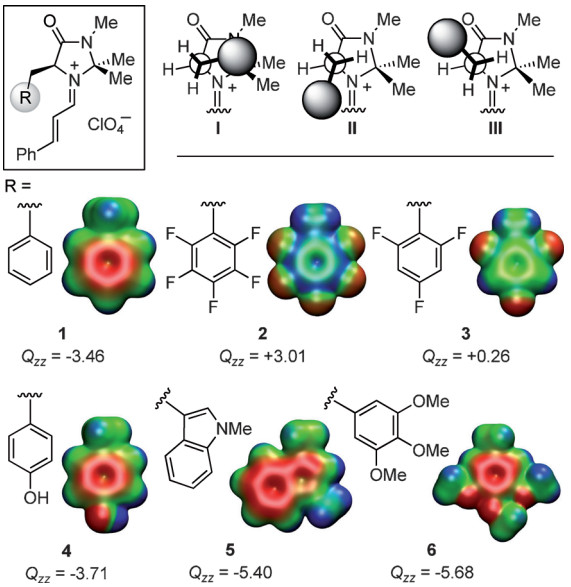

Figure 2. Top: Three possible low-energy conformers of imidazolidinone-derived α,β-unsaturated iminium salts **1**–**6** (**I** = CH–π; **II** = π–π). Bottom: The components of the traceless quadrupole moment tensor orthogonal to the aromatic ring (Debeye–Ångstrom, Q_{zz}) are given for the corresponding toluene derivatives (i.e. $ArCH_3$). Q_{zz} calculated using DFT (TPSS/def2-TZVP). Electrostatic potential maps (ESP) of the substituted toluene derivatives corresponding to **1**–**4**, and **6** and the methyl indole derivative corresponding to **5**. Isosurfaces correspond to an electron density of 0.005 a.u. Color range of the electrostatic potential: −0.02 (red) to +0.05 (blue).

electrostatic potential map (ESP) as shown in Figure 2. Gratifyingly, it was possible to isolate and crystallize an electron-deficient (**2**ClO_4^-, R = C_6F_5) and an electron-rich example (**4**ClO_4^-, R = C_6H_4OH) to compare solid-state conformations with that of **1**.[9f]

The effect of electronic modulation was immediately evident on the conformation. Of the three staggered conformations indicated in Figure 2 (**I**–**III**), the electron-rich phenylalanine derivative **1** (R = Ph) resided in conformation **I**, a trend that was preserved in the tyrosine derivative **4** (R = C_6H_4OH; Figure 3, right).[13] In contrast, the electron-deficient pentafluorophenyl analogue **2** (R = C_6F_5) adopted conformation **III** (Figure 3, left) such that the aryl group lies proximal to the C=O unit of the imidazolidinone (φ_{CCCC} = +31°).[14] Houk and co-workers calculated the staggered conformer corresponding to **III** (crotonaldehyde derivative when R = Me, **1**)[11] to be energetically unfavorable. Moreover, Seebach and Grimme have calculated that this species is not an energy minimum at all in their "windshield-wiper model".[15] To the best of our knowledge structural data for systems with this conformation have so far not been reported.

To complement this crystallographic study, a detailed spectroscopic investigation was performed, including a conformer population analysis. The mole fractions (X_I, X_{II}, and X_{III}) of the electron-rich species **1** and **4**–**6**, and the electron-deficient systems **2** and **3** were derived from the ^3J coupling constants ($ArCH_2$ and 5-H) using the Diez–Altona–Donders equation[16] with the aid of MestReJ v1.1.[17] It was assumed that only staggered rotamers with dihedral angles of 60° contribute to ^3J (**I**–**III**, Table 1). From this analysis it is evident that electron-rich species such as **1**, **4**, **5**, and **6** predominantly populate conformer **I** at room temperature. The remaining 25–40% are divided between **II** and **III**. Notably, in more electron-rich species such as **5** and **6** conformer **II** is populated more by 28% and 17%, respectively. In the parent system **1**, conformer **II** is essentially unpopulated at rt. As expected, the electron-deficient pentafluorophenyl system **2** does not predominantly populate conformation **I** at room temperature, but instead shows a more varied distribution favoring **II** and **III** (roughly 60% overall). This tendency is preserved in species **3**. These trends can also be derived from the ^1H and ^{13}C chemical shifts of the *gem*-dimethyl groups of these iminium salts (Table 1, right). Whilst the large Δδ(*syn*/*anti*) values in the ^1H NMR spectra of iminium salts **1** and **4**–**6** (Δδ = 0.58–0.89 ppm) can be attributed to the shielding of the *syn*-methyl protons in conformer **I**, the small Δδ(*syn*/*anti*) values in **2** and **3** are indicative of the small population of

Table 1: Conformational analysis of **1**–**6**; calculation of the mole fractions X_I, X_{II}, and X_{III} at room temperature in MeCN.[a]

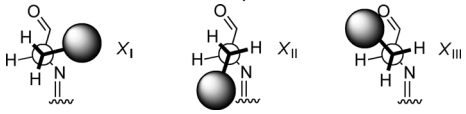

Iminium salt	Q_{zz}	Mole fractions			$\Delta\delta_{(syn/anti)}$	
		X_I	X_{II}	X_{III}	^1H	^{13}C
2	+3.01	0.37	0.16[b]	0.47[b]	−0.13	+0.36
3	+0.26	0.39	0.21[c]	0.40[c]	−0.18	+0.06
1	−3.46	0.75	0.03	0.23	−0.89	−2.77
4	−3.71	0.76	0.04	0.20	−0.78	−2.48
5	−5.40	0.57	0.28	0.15	−0.58	−1.68
6	−5.68	0.65	0.17	0.18	−0.62	−1.87

[a] NMR spectra were recorded on an Agilent DD2 500 or 600 MHz spectrometer (room temperature, MeCN). The benzylic protons were individually assigned by NOE analysis. [b,c] Due to the absence of a significant HF heteronuclear NOE these values could be interchanged ($X_{II} + X_{III} \approx 60\%$).

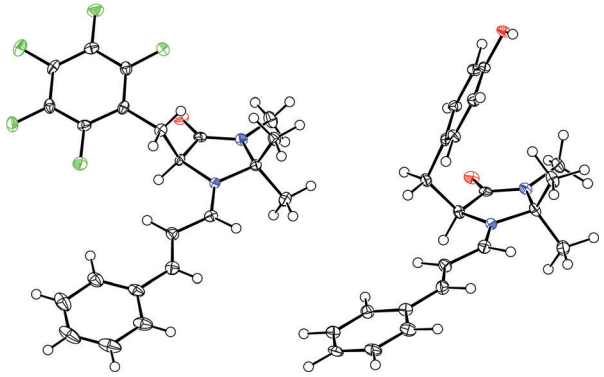

Figure 3. X-ray crystal structures of iminium salts **2** (conformer **III**) and **4** (conformer **I**). Thermal ellipsoids shown at the 50% probability level; the ClO_4^- counterions have been omitted for clarity; gray C, green F, blue N, red O.[13,14]

conformer **I** in these electron-deficient species. Similar conclusions can also be drawn from the ^{13}C NMR spectra.

In order to examine how the electronic nuances of the aryl groups influence the electrophilic reactivities of the iminium salts, we have studied the kinetics of the reactions of the most electron-deficient (**2**) and the most electron-rich (**6**) species with ketene acetals **7** and **8**, which have previously been employed as reference nucleophiles. Previous work has established that the reactions of carbocations and Michael acceptors with σ, *n*, and π nucleophiles follow Equation (1), in

$$\log\ k_2\ (20\,^{\circ}\mathrm{C}) = s_N\ (E + N) \qquad (1)$$

which electrophiles are described by *E* (electrophilicity parameter) and nucleophiles are described by *N* (nucleophilicity parameter) and s_N (nucleophile-specific sensitivity parameter).[18]

Using this approach it has been possible to establish comprehensive electrophilicity and nucleophilicity scales covering more than 30 orders of magnitude. Recently, the reactivities of imidazolidinone-derived iminium salts have been shown to fit Equation (1) perfectly.[19] Now, the kinetics of the reactions of **2** and **6** with silyl ketene acetals **7** and **8** were followed photometrically in CH_2Cl_2 at 20 °C by monitoring the decay of the absorbances of **2** and **6** at 376 nm and 374 nm, respectively.

By using the nucleophiles **7** and **8** in large excess, pseudo-first-order kinetics were achieved, and the first-order rate constants k_{obs} (s^{-1}) were derived from the exponential decays of the iminium salts **2** and **6** (Figure 4). Plots of k_{obs} versus the concentrations of the nucleophiles (Figure 4) were linear, with the second-order rate constants k_2 ($M^{-1}s^{-1}$) as slopes. The electrophilicity parameters (Table 2) show that **2** is about 9 times more reactive than **6**, exhibiting comparable reactivity to that of the iminium salt derived from MacMillan's second-generation catalyst (Figure 5).

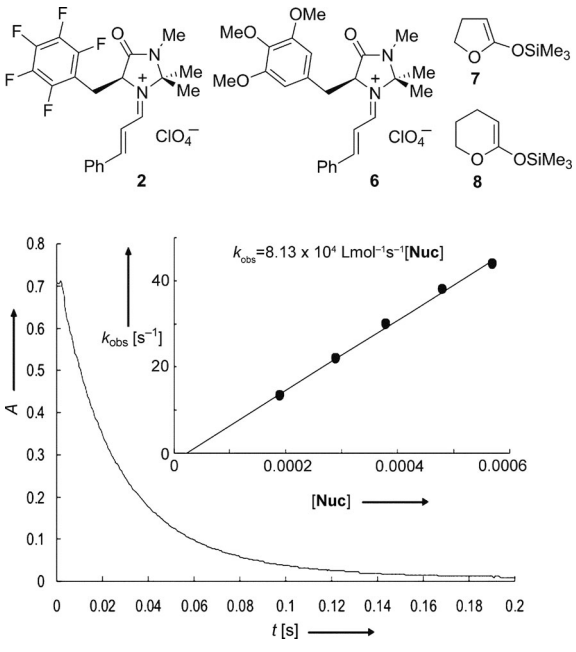

Figure 4. Exponential decay of the absorbance at 376 nm during the reaction of **6**ClO_4^- (9.55×10^{-6} M) with **7** (5.70×10^{-4} M). Inset: Determination of the second-order rate constant k_2 from the dependence of the first-order rate constant k_{obs} for the reaction of **2**ClO_4^- with **7** on the concentration of ketene acetal **7** (20 °C in CH_2Cl_2). Nuc = nucleophile.

Table 2: Second-order rate constants k_2 for the reactions of the iminium salts **1**, **2**, and **6** with the ketene acetals **7** and **8** (20 °C, CH_2Cl_2, counterion: ClO_4^-).

	k_2 (**7**) [$M^{-1}s^{-1}$]	k_2 (**8**) [$M^{-1}s^{-1}$]	E[a]
1[b]	9.06×10^3	5.23×10^2	−7.2[c]
2	8.13×10^4	3.43×10^3	−6.0
6	1.49×10^4	5.78×10^2	−7.0

[a] The *E* parameters for **2** and **6** were determined from a least-squares minimization of $\Delta^2 = \Sigma(\log\ k_2 - s_N(E+N))^2$ which uses the second-order rate constants k_2 (this table) and the nucleophile parameters *N* and s_N (for **7**: $N = 12.56$, $s_N = 0.70$; for **8**: $N = 10.61$, $s_N = 0.86$).[18] [b] OTf^- counterion [c] Ref. [19a].

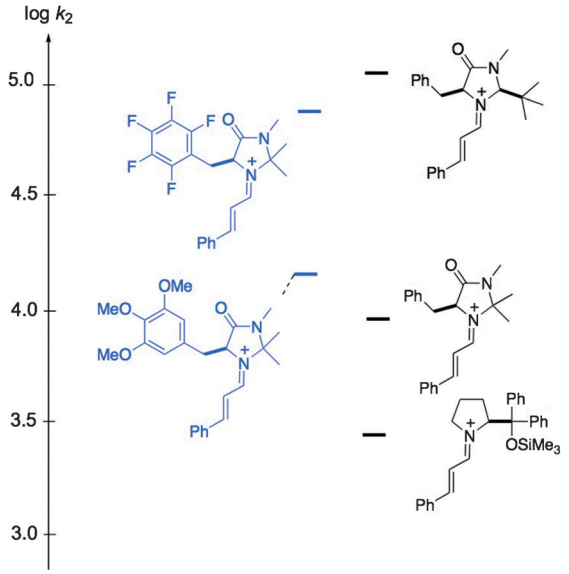

Figure 5. Comparison of the relative second-order rate constants for the reactions of the iminium ions **2** and **6** with the ketene acetal **7** in CH_2Cl_2 at 20 °C. The second-order rate constant for the reaction of the iminium ion derived from MacMillan's second-generation catalyst with the ketene acetal **7** is taken from Ref. [19b].

However, the presence of three methoxy groups at the phenyl ring of the imidazolidinone had little effect on the electrophilicity of the iminium system; the reactivity profile of **6** was comparable to that of MacMillan's first-generation catalyst (Figure 5).

Finally, to explore the behavior of the modified imidazolidinones in catalysis, the Friedel–Crafts reaction of *N*-methylpyrrole (**9**) with *trans*-cinnamaldehyde (**10**) was examined (Figure 6).[20] To this end, only the substituted benzene derivatives were screened for direct comparison of substituent effects. Reactions were performed in THF/H_2O at ambient temperature, using 20 mol% catalyst loading, and

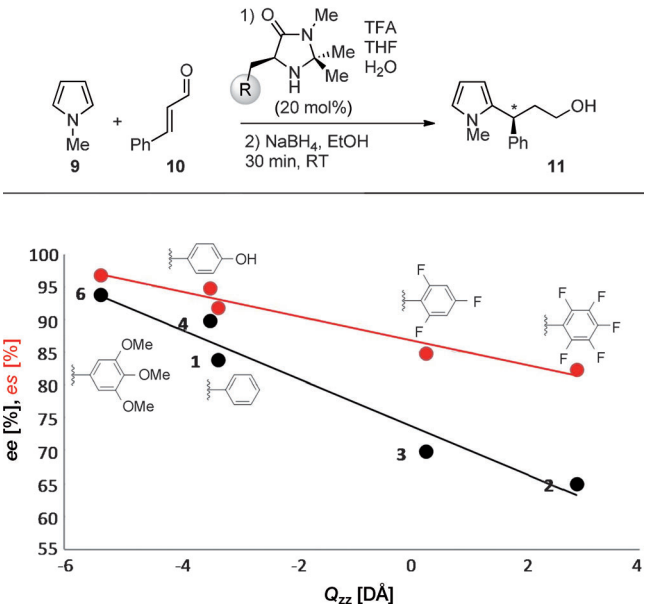

Figure 6. Top: Organocatalytic Friedel–Crafts alkylation of *N*-methylpyrrole (**9**) and *trans*-cinnamaldehyde (**10**). Bottom: Correlation of the component of the traceless quadrupole moment tensor orthogonal to the aromatic ring of the $ArCH_3$ derivatives (Q_{zz}) with enantiomeric excess (*ee*), and enantioselectivity (*es*).

the enantioselectivities of the corresponding alcohols (**11**) following in situ reduction were measured. In view of the counterion dependence of this reaction, the TFA salts were used throughout.[21]

All catalysts proved to be highly competent, with reactions reaching completion in 3 h. Intriguingly, a direct correlation was observed between the quadrupole moment of the arene moiety Q_{ZZ} and the enantioselectivity (*es*) of the reaction (Figure 6, bottom). Whilst the electron-deficient species (R = C_6F_5 and $C_6H_2F_3$, corresponding to **2** and **3**, respectively) gave moderate levels of enantioinduction (65 and 70% *ee*, respectively), the more electron-rich system proceeding via iminium salt **1** gave marked improvements in enantioselectivity (R = Ph, 84% *ee*). Moreover, the tyrosine derivative furnished the product alcohol **11** in 90% *ee*. Particularly noteworthy is the trimethoxy derivative which allowed this transformation to be completed at ambient temperature in 3 h (94% *ee*) as opposed to 42 h at −30 °C (93% *ee*) as initially reported.[20]

Herein we verify that electronic modulation of the shielding group in the MacMillan catalyst (as a function of Q_{zz}) influences the ground-state conformer population of the corresponding α,β-unsaturated iminium salts. In addition, changes in the aryl group were found to modulate reactivity. Whilst iminium salt **6** displayed comparable reactivity to the parent species, the pentafluorophenyl derivative was around 9 times more reactive, thus making it comparable to the MacMillan second-generation catalyst.[19b,22] Finally, the competence of the parent imidazolidinones was investigated in the Friedel–Crafts reaction of *N*-methylpyrrole with *trans*-cinnamaldehyde (Figure 6). A direct correlation between the component of the traceless quadrupole moment tensor orthogonal to the aromatic ring (Q_{ZZ}) and the enantioselectivity of this transformation was identified. Application of the electron-rich 3,4,5-trimethoxy derivative allowed the reaction to be performed in 3 h rather than 42 h, and at ambient temperature rather than −30 °C, with comparable levels of enantiocontrol. This preliminary study has established that modulating the shielding group electronics of the imidazolidinone has a number of practical advantages for future catalyst development. Systems which are predisposed to participate in CH–π interactions or interact with the pendant iminium chain facilitate enantioinduction. This trend may be a consequence of the enhanced capability of electron-rich aryl groups to participate in stabilizing cation–π-type interactions[23] in the enantio-determining transition state. A recent theoretical study at the MP2 level demonstrates the importance of this interaction in stabilizing conformer **II**.[24]

We envisage that a careful examination of these ephemeral noncovalent interactions will assist in predicting reaction outcomes and formulating guidelines for future catalyst development.

Received: March 5, 2013
Revised: April 4, 2013
Published online: June 21, 2013

Keywords: conformational analysis · fluorine · imidazolidinone · kinetics · organocatalysis

[1] *Asymmetric Organocatalysis: From Biomimetic Concepts to Applications in Asymmetric Synthesis* (Eds.: A. Berkessel, H. Gröger), Wiley-VCH, Weinheim, **2005**.
[2] a) J. R. Knowles, *Nature* **1991**, *350*, 121 – 124; b) R. R. Knowles, E. N. Jacobsen, *Proc. Natl. Acad. Sci. USA* **2010**, *107*, 20678 – 20685.
[3] J.-M. Lehn, *Science* **1993**, *260*, 1762 – 1763.
[4] D. W. C. MacMillan, *Nature* **2008**, *455*, 304 – 308.
[5] K. A. Ahrendt, C. J. Borths, D. W. C. MacMillan, *J. Am. Chem. Soc.* **2000**, *122*, 4243 – 4244.
[6] a) M. Brandl, M. S. Weiss, A. Jabs, J. Sühnel, R. Hilgenfeld, *J. Mol. Biol.* **2001**, *307*, 357 – 377; b) O. Takahashi, Y. Kohono, M. Nishio, *Chem. Rev.* **2010**, *110*, 6049 – 6076.
[7] G. B. McGaughey, M. Gagné, A. K. Rappé, *J. Biol. Chem.* **1998**, *273*, 15458 – 15463.
[8] For the X-ray structure of the MacMillan first-generation catalyst see: J. C. Burley, R. Gilmour, T. J. Prior, G. M. Day, *Acta Crystallogr. Sect. C* **2008**, *64*, o10 – o14.
[9] For selected examples see: a) D. Seebach, U. Grošelj, M. D. Badine, W. B. Schweizer, A. K. Beck, *Helv. Chim. Acta* **2008**, *91*, 1999 – 2034; b) U. Grošelj, W. B. Schweizer, M.-O. Ebert, D. Seebach, *Helv. Chim. Acta* **2009**, *92*, 1 – 13; c) J. B. Brazier, G. Evans, T. J. K. Gibbs, S. J. Coles, M. B. Hursthouse, J. A. Platts, N. C. O. Tomkinson, *Org. Lett.* **2009**, *11*, 133 – 136; d) D. Seebach, R. Gilmour, U. Grošelj, G. Deniau, C. Sparr, M.-O. Ebert, A. K. Beck, L. B. McCusker, D. Sisak, *Helv. Chim. Acta* **2010**, *93*, 603 – 634; e) C. Sparr, R. Gilmour, *Angew. Chem.* **2010**, *122*, 6670 – 6673; *Angew. Chem. Int. Ed.* **2010**, *49*, 6520 – 6523; f) C. Sparr, R. Gilmour, *Angew. Chem.* **2011**, *123*, 8541 – 8545; *Angew. Chem. Int. Ed.* **2011**, *50*, 8391 – 8395; g) For an excellent review of theoretical investigations of organocatalysis see: P. H.-Y. Cheong, C. Y. Legault, J. M. Um, N. Çelebi-Ölçüm, K. N. Houk, *Chem. Rev.* **2011**, *111*, 5042 – 5137, and references therein.

[10] M. Nishio, M. Hirota, Y. Umezawa, *The CH/π Interaction*: *Evidence*, *Nature and Consequences*, Wiley-VCH, Weinheim, **1998**.
[11] R. Gordillo, J. Carter, K. N. Houk, *Adv. Synth. Catal.* **2004**, *346*, 1175 – 1185.
[12] For examples from this laboratory see: C. Sparr, W. B. Schweizer, H. M. Senn, R. Gilmour, *Angew. Chem.* **2009**, *121*, 3111 – 3114; *Angew. Chem. Int. Ed.* **2009**, *48*, 3065 – 3068, and references [9f] and [11].
[13] 925388 contains the supplementary crystallographic data for this paper. These data can be obtained free of charge from The Cambridge Crystallographic Data Centre via www.ccdc.cam.ac.uk/data_request/cif.
[14] 925387 contains the supplementary crystallographic data for this paper. These data can be obtained free of charge from The Cambridge Crystallographic Data Centre via www.ccdc.cam.ac.uk/data_request/cif.
[15] D. Seebach, U. Grošelj, W. B. Schweizer, S. Grimme, C. Mück-Lichtenfeld, *Helv. Chim. Acta* **2010**, *93*, 1 – 16.
[16] a) C. Altona in *Encyclopedia of NMR* (Eds.: D. M. Grant, R. Morris), Wiley, New York, **1996**; b) E. Díez, J. San-Fabián, J. Guilleme, C. Altona, L. A. Donders, *Mol. Phys.* **1989**, *68*, 49 – 63.
[17] A. Navarro-Vazquez, J. C. Cobas, F. J. Sardina, *J. Chem. Inf. Comput. Sci.* **2004**, *44*, 1680 – 1685.
[18] H. Mayr, T. Bug, M. F. Gotta, N. Hering, B. Irrgang, B. Janker, B. Kempf, R. Loos, A. R. Ofial, G. Remennikov, H. Schimmel, *J. Am. Chem. Soc.* **2001**, *123*, 9500 – 9512.
[19] a) S. Lakhdar, T. Tokuyasu, H. Mayr, *Angew. Chem.* **2008**, *120*, 8851 – 8854; *Angew. Chem. Int. Ed.* **2008**, *47*, 8723 – 8726; b) S. Lakhdar, J. Ammer, H. Mayr, *Angew. Chem.* **2011**, *123*, 10127 – 10130; *Angew. Chem. Int. Ed.* **2011**, *50*, 9953 – 9956; c) H. Mayr, S. Lakhdar, B. Maji, A. R. Ofial, *Beilstein J. Org. Chem.* **2012**, *8*, 1458 – 1478.
[20] N. A. Paras, D. W. C. MacMillan, *J. Am. Chem. Soc.* **2001**, *123*, 4370 – 4371.
[21] S. Lakhdar, H. Mayr, *Chem. Commun.* **2011**, *47*, 1866 – 1868.
[22] J. F. Austin, D. W. C. MacMillan, *J. Am. Chem. Soc.* **2002**, *124*, 1172 – 1173.
[23] a) J. C. Ma, D. A. Dougherty, *Chem. Rev.* **1997**, *97*, 1303 – 1324; b) J. P. Gallivan, D. A. Dougherty, *Proc. Natl. Acad. Sci. USA* **1999**, *96*, 9459 – 9464; c) L. M. Salonen, M. Ellermann, F. Diederich, *Angew. Chem.* **2011**, *123*, 4908 – 4944; *Angew. Chem. Int. Ed.* **2011**, *50*, 4808 – 4842.
[24] Y. Mori, S. Yamada, *Molecules* **2012**, *17*, 2161 – 2168.

